Journal of Civil Engineering and Architecture 18 (2024) 261-268 doi: 10.17265/1934-7359/2024.06.001



Proposal of a Method to Easily Understand Rainfall Infiltration in Railway Embankments

Takashi Nakayama¹, Tadashi Hara² and Keigo Koizumi³

- 1. C. S. Inspector Co., Ltd., 2-7-2 Nambanaka Naniwa-Ku Osaka-Shi, Osaka-Fu 556-0011, Japan
- 2. Research and Education Faculty, Kochi University, 2-5-1 Akebonocho Kochi-Shi, Kochi-Ken 780-8072, Japan
- 3. Earth Watch Institute, Inc., 8-10 Toyotsucho Suita-Shi, Osaka-Fu 564-0051, Japan

Abstract: Slope failures due to heavy or prolonged rain have been occurring frequently in Japan in recent years. In railway embankments, even small-scale surface collapse can result in track deformation. Currently, train operation during rainy periods is regulated according to empirical rules based on rainfall and disaster history. However, the validity of operation regulations is lacking because the rainfall infiltration circumstances inside the slope are unknown. We have been attempting to understand rainfall infiltration in railway embankments by applying a method of predicting surface collapse from observations of volumetric water content in the soil. We used previous field monitoring and model experiments to propose a method for easily understanding the state of rainfall infiltration in the surface layer of an embankment using the relative history of volumetric water content at different depths. In this study, we applied this simple determination method to railway embankments with different topography and geological environments to demonstrate the versatility of the method.

Key words: Railway embankments, field monitoring, volumetric water content.

1. Introduction

Heavy and prolonged rain has globally increased in frequency in recent years due to the impacts of climate change, which has increased the risk of landslides. For railways in Japan, over 80% of the civil engineering structures are earthen, such as embankments, with many built in ancient times. Such embankments have lower performance and quality than those constructed in recent years due to their manual construction and the lack of use of high-quality embankment materials [1].

If slope failure occurs above the railway, then train service can be resumed even if earth and sand flow into the tracks as the debris can be removed as an emergency measure. However, in the case of embankment collapse, the ground needs to be rebuilt, resulting in a long recovery time [2]. Additionally, the result of statistical analysis of railway embankment cases showed that even when collapses reach the top of a slope, the

thickness is often ≥ 1 m and < 2 m [3]. This indicates that railway embankments in Japan are at risk of track deformation with even a small-scale surface collapse, which would result in the suspension of train service for a long time.

Railway embankments are collapsing due to heavy rain even in Europe, where railways have been developed for a long time. The most recent incidents occurred in Hampshire, England in January 2024 [4] and Shropshire, England in March 2024 [5], resulting in long-term train service suspensions. Additionally, in Sweden, an accident occurred in August 2023 in which a train derailed due to an embankment collapse [6], and thus countermeasures against heavy rains in railway embankments are an urgent issue.

The soundness of railway embankments in Japan is evaluated by visual inspection [7]. Such evaluations use qualitative judgments, such as the presence or absence of spring water at the toe of a slope or the presence or

Corresponding author: Takashi Nakayama, Master of Engineering (Civil Engineering), research fields: railway engineering, slope, field monitoring.

absence of concentrated water flowing down a slope face. Furthermore, during rainfall, empirical rules based on hourly and continuous rainfall during past disasters are used to regulate operations [8]. However, these methods often do not show the infiltration conditions that cause collapse, such as rainfall infiltration, rise in the saturated zone, generation of pore water pressure, and surface displacement, and the validity of their judgments is often unclear. In Japan, there are high social demands for safe and on-time operation, and management methods need to be reviewed.

Koizumi et al. [9] proposed a method for monitoring the volumetric water content of the surface layer of a slope and predicting the risk of surface layer failure. Fig. 1 shows a schematic diagram of the results of a small laboratory model experiment. Soil moisture meters were buried at three depths. The volumetric water content of the soil increases from depths close to the ground surface due to vertical rainfall infiltration. However, before the formation of a saturated zone at the interface with the base layer, a quasi-saturated state is created in which the volumetric water content temporarily reaches equilibrium. The volumetric water content at this time is called the IQS (initial quasisaturated volumetric water content). Observing the point at which IQS is reached may enable the prediction of deformation due to rainfall. IQS indicates a state in which the amount of inflow from above and runoff from below are temporarily balanced in the vertical rainfall infiltration at any point on a slope.

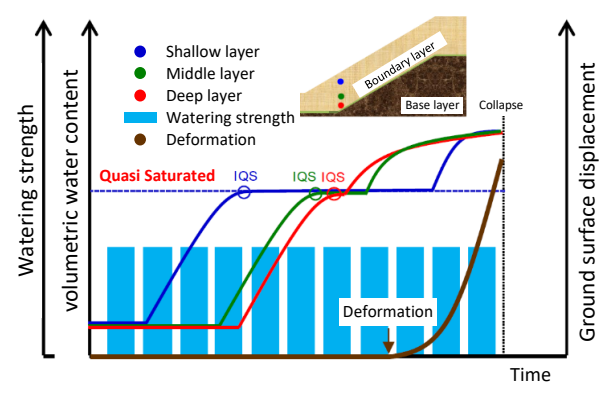


Fig. 1 Relationship between infiltration characteristics and IQS based on slope model experiments [9].

We have attempted to understand the rainfall infiltration status from the volumetric water content of the slope surface layer in a railway embankment (hereinafter, site A), which is a cut and fill embankment, by applying the IQS concept [10-12]. We propose a method that uses the initial quasi-saturated volumetric water content on descent (D-IQS), which is an approximation of IQS, to easily understand the rainfall infiltration status in the surface layer of an embankment in real-time using the relative history of changes in two volumetric water contents at different depths. In this study, we applied this simple determination method used in site A to a railway embankment with a different topography and geological environment (hereinafter, site B) to demonstrate the versatility of the method.

2. Overview of Field Monitoring Sites and Observation Methods

In this study, we sought to understand the rainfall infiltration in the railway embankment surface layer through field monitoring of the volumetric water content in the slope surface layer by selecting two sites with different topography and sedimentary environments (site A, site B), where we conducted field monitoring of the volumetric water content [13] from October 2020. Site A is a cut and fill embankment parallel to the coastline. Site A ground surveys [10] and field monitoring [11] as well as column model experiments [12] showed that the thickness of the embankment layer on the slope was approximately 1 m at the top of the slope and toe of the slope and approximately 2 m at the mid-slope, indicating not only infiltration in the vertical direction on the slope surface but also the lateral flowing of the rain that fell on the track area. Fig. 2 shows the location map of site B. It is a cut and fill embankment located in a mountainous area, with single-track operation beginning in the 1920s and being converted to doubletrack operation in the 1960s. A nearby widening of embankment collapsed several years ago due to heavy rain. Spring water could be seen at the toe of the slope during rainfall, with small-scale collapses having occurred



Fig. 2 Site B location map.

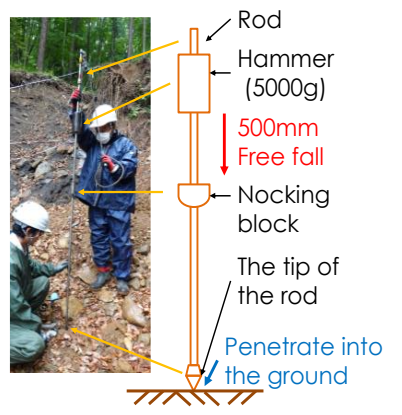


Fig. 3 Overview of PDCP (portable dynamic cone penetration).

halfway up the slope face in the past. The observation point was halfway up the slope face and was close to a natural slope.

We sought to understand the sedimentation status of the local ground and plan the installation location of the soil moisture meter by conducting a PDCP test, which is a simple method for investigating the relative softness of the soil. Fig. 3 shows an overview of the PDCP. This is a type of sounding that determines the softness of the ground by free-falling a hammer with a mass of 5 kg from a height of 0.5 m and using the number of strikes N_d required to penetrate the tip of the rod by 0.1 m into the ground. Fig. 4 shows the crosssectional shape of site B, an example of the PDCP results, the geological boundaries assumed from the PDCP depths of $N_{\rm d}$ < 10 and $N_{\rm d}$ < 20, and the installation status of soil moisture meters. The soil at the site where the soil moisture meter is installed was coarse-grained soil with a wide range of grain sizes, but the fine-grain content F_c was 35%-52% and had low water permeability, and the degree of compaction Dc at the site was no more than 70%, and therefore it was significantly lower than the current design standard (at least 90%) [14]. The depths of $N_d < 10$ and $N_d < 20$ obtained by PDCP were almost identical, and there was a clear difference in the softness and hardness of the ground, and thus it was thought that this corresponded to the geological boundary between the topsoil layer and base layer. In this study, we sought to understand the influence of differences in permeability on rainfall infiltration by setting the surface collapse above this boundary as the observation target and burying soil moisture meters (SM-150T, manufactured by Delta-T) at three depths in two locations (ID3 and ID4 in the figure) halfway up the slope face. ID3 has a thinner topsoil layer thickness than ID4. We installed a rain gauge and inclinometer, used LPWA (Low Power Wide Area) for data communication, and performed continuous recording at 15-min intervals.

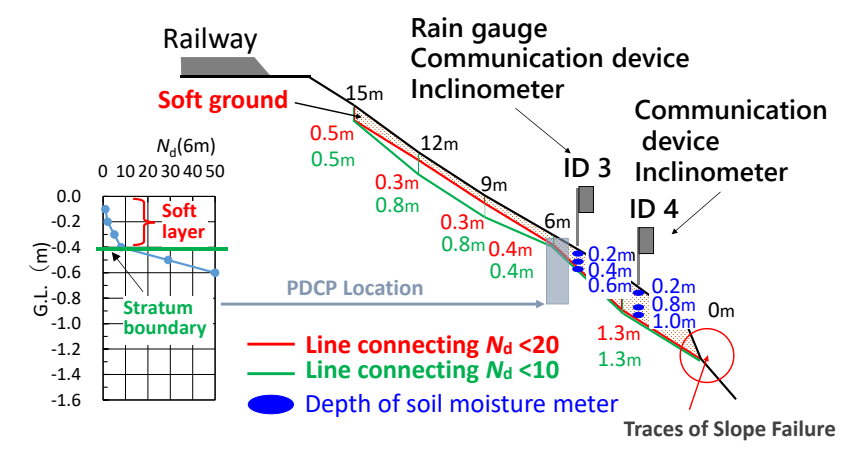


Fig. 4 Cross-sectional view of site B and equipment installation status.

3. Field Monitoring Results of Volumetric Water Content Using Soil Moisture Meter

We continuously observed volumetric water content at the site from October 2020 to August 2023. We discuss the results for ID3 and ID4.

In ID3, there were 52 events during the observation period with an increase in the volumetric water content at G.L.-0.6 m near the strata boundary. None of these events exhibited the formation of a saturated zone after the quasi-saturated state seen in the model experiment results of Koizumi et al. [9] (i.e., a state in which equilibrium was reached in IQS). Additionally, fluctuations in volumetric water content that were different from vertical infiltration were observed. Fig. 5 shows the change in volumetric water content over time, showing vertical infiltration. The volumetric water content increased in the order of G.L.-0.2 m (blue), which was close to the ground surface, G.L.-0.4 m (green), and G.L.-0.6 m (red), and the start times of the increase were almost equally spaced and proportional to the depth, suggesting that vertical infiltration occurred. Fig. 6 shows the change over time in volumetric water content above the strata boundary, where lateral inflow was thought to have occurred. After the increase in G.L.-0.2 m, there was an increase in G.L.-0.6 m, which is close to the strata boundary, at an earlier stage than at G.L.-0.4 m, and unlike in Fig. 5, it is thought that there was lateral inflow along the strata boundary. Fig. 7 shows the temporal change in volumetric water content that is thought to have exceeded IQS near G.L.-0.6 m and reached saturation. The volumetric water content showed a steady state at approximately 53%, and then rapidly decreased due to the decrease in rainfall, which was similar to the fluctuation at site A during saturation.

Meanwhile, in ID4, there were 24 events during the observation period with an increase in volumetric water content at G.L.-1.0 m. Only one of these events exhibited the formation of a saturated zone after equilibrium was reached in IQS. Fig. 8 shows the change

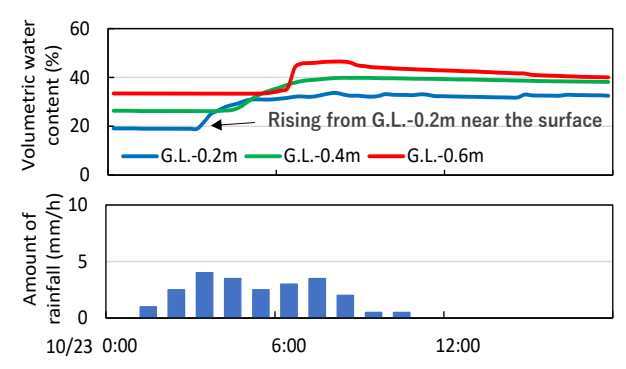


Fig. 5 Change over time in volumetric water content 10/23/2020 (ID3 vertical infiltration case).

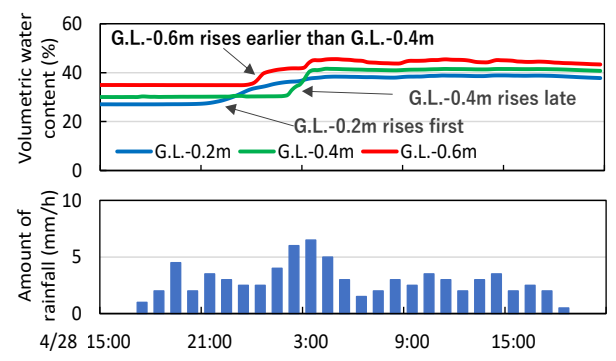


Fig. 6 Change over time in volumetric water content 4/28/2021 (ID3: lateral inflow case).

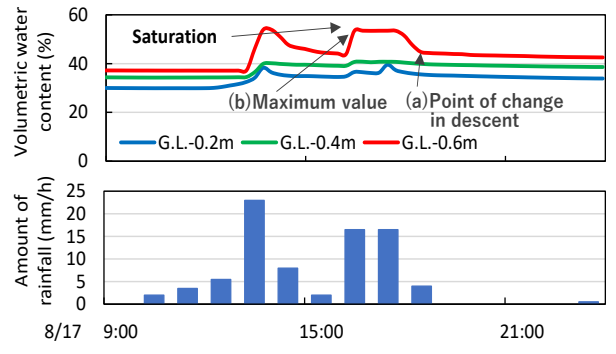


Fig. 7 Change over time in volumetric water content 8/17/2021 (ID3 saturation case).

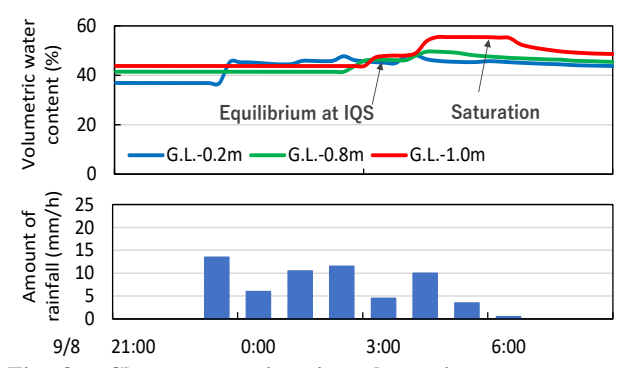


Fig. 8 Change over time in volumetric water content 9/9/2021 (ID4 saturation case after equilibration at IQS).

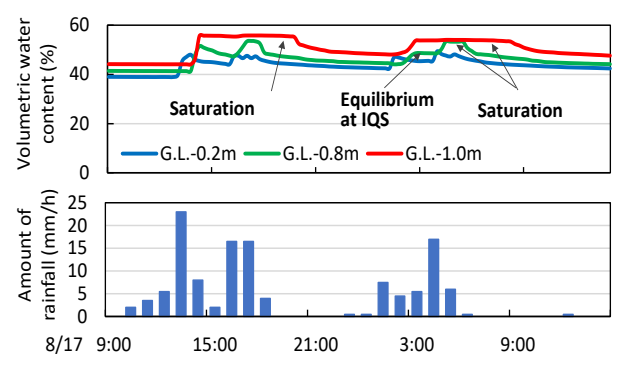


Fig. 9 Change over time in volumetric water content 8/17/2021 (ID4 saturation case).

over time here. After the increase at G.L.-0.2 m, there was an increase in the order of G.L.-0.8 m and G.L.-1.0 m, with equilibrium being reached in IQS. Afterwards, there were almost simultaneous increases again at G.L.-0.8 m and G.L.-1.0 m, with G.L.-1.0 m believed to have reached saturation at a volumetric water content at approximately 55%. Fig. 9 shows the temporal change in volumetric water content that is believed to have reached saturation at both G.L.-0.8 m and G.L.-1.0 m. The value at G.L.-0.8 m shows a steady state when the volumetric water content is at approximately 53%, and the value at G.L.-0.8 m shows a steady state when the volumetric water content is at approximately 54%. Additionally, in ID4, there were cases where vertical penetration appeared as shown in Fig. 5, and cases where the volumetric water content at deep positions rose earlier than at shallower positions, as shown in Fig. 6.

The following rainfall infiltration could be inferred based on the above observation results.

- (a) Both ID3 and ID4 exhibited vertical infiltration as well as lateral inflow, and it was inferred that the inflow was from the railway line.
- (b) ID3 exhibited saturation due to lateral inflow only at G.L.-0.6 m near the strata boundary, and it was inferred that the infiltrated rainfall flowed downward along the strata boundary.
- (c) ID4 reached saturation in the order of G.L.-1.0 m and G.L.-0.8 m, and the saturated zone rose from the strata boundary. It was inferred that, if the water level occurred near the strata boundary and the saturated

zone rose further, then collapse may occur due to the decrease in effective stress.

(d) Only one case in ID4 exhibited the formation of a saturated zone after reaching an equilibrium state in IQS, and IQS was difficult to estimate from field monitoring.

4. Verification of Simple Method for Determining Rainfall Infiltration Conditions for Railway Embankment

We compared the rainfall infiltration situation estimated using a simple discriminant diagram with the rainfall infiltration situation estimated in Section 3 to verify the versatility of the discriminant diagram-based determination method. IQS has also conventionally been used as a threshold for understanding the rainfall infiltration situation [9]. However, no clear IQS was observed at site B, and thus the D-IQS used at site A was used as the threshold.

4.1 Rainfall Infiltration Status Discriminant Diagram

First, we discuss ID3. Fig. 10 plots the intersection point of the (a) volumetric water content at the point of change in descent and the (b) maximum volumetric water content (example shown in the graph in Fig. 7) for the 23 rainfall events in which the area around G.L.-0.6 m seemed to have reached IOS. At G.L.-0.6 m, the (a) volumetric water content at the point of change in descent converged in the range of 42%-45%, regardless of the (b) maximum volumetric water content, and thus D-IQS was estimated as 44% using the average value. At G.L.-0.4 m, the (a) volumetric water content at the point of change in descent and the (b) maximum volumetric water content was almost equivalent and did not reach a quasi-saturated state. Fig. 11 shows the transition history by plotting the intersection of the volumetric water content of G.L.-0.4 m and G.L.-0.6 m at a certain time and connecting them with a straight line. For G.L.-0.6 m, D-IQS (44%) was the threshold. For G.L.-0.4 m, both IOS and D-IOS were unclear, and thus the maximum observed value (43%) was set as the

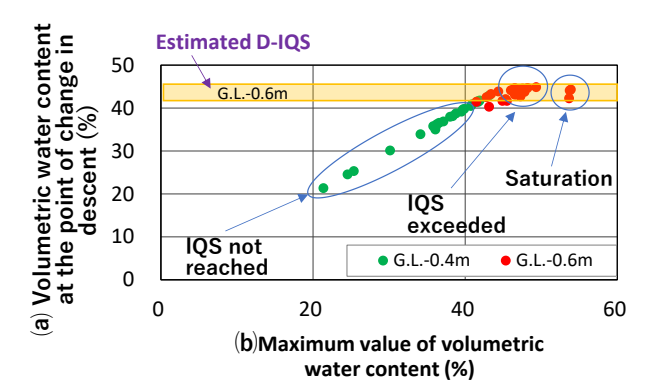


Fig. 10 Estimation graph of D-IQS (ID3).

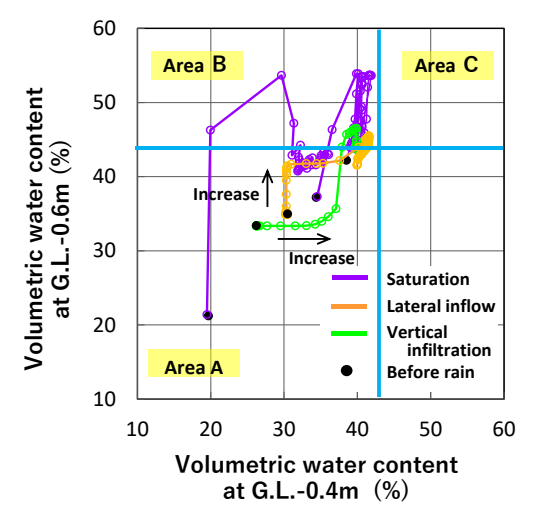


Fig. 11 Rainfall infiltration status discrimination graph (ID3).

threshold. These thresholds were shown as blue lines, and the graph was divided into the three areas A-C. The yellow-green line indicates the vertical infiltration shown in Fig. 5, and after the G.L.-0.4 m value increased in area A, the G.L.-0.6 m value increased, after which it took a trajectory toward area B. The orange line indicates the lateral inflow shown in Fig. 6, and after the G.L.-0.6 m increased in area A, the G.L.-0.4 m value increased, after which it took a trajectory toward area B. The purple line in the figure represents three rainfall events that reached saturation, including that shown in Fig. 7, moving from area A to area B, but not reaching area C.

Next, we discuss ID4. Fig. 12 plots the (a) volumetric water content at the point of change in descent and (b) maximum volumetric water content for the nine rainfall events in which the area around G.L.-1.0 m seemed to

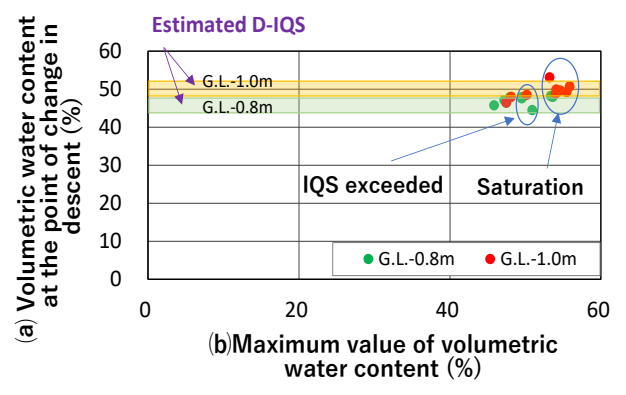


Fig. 12 Estimation graph of D-IQS (ID4).

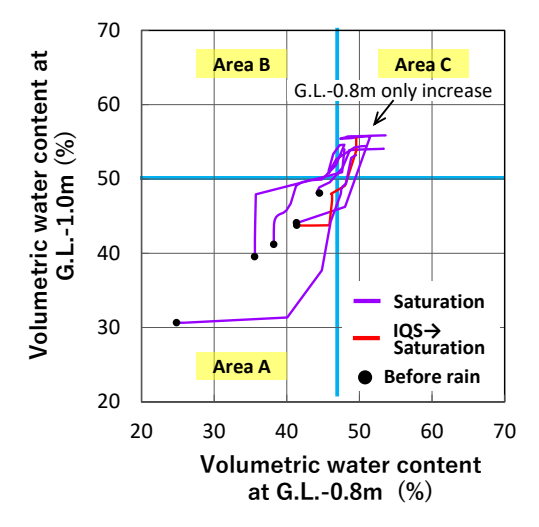


Fig. 13. Rainfall infiltration status discrimination graph (ID4).

have reached IQS. The (a) volumetric water content at the point of change in descent converged to a range of 46%-48% at G.L.-0.8 m and 46%-53% at G.L.-1.0 m. We used average values to estimate the D-IQS at G.L.-0.8 m to be 47% and the D-IQS at G.L.-1.0 m to be 50%. Fig. 13 shows the transition history by plotting the intersection of the volumetric water content of G.L.-0.8 m and G.L.-1.0 m at a certain time from before the rain to (b) the maximum value of the volumetric water content, and connecting them with a straight line. D-IQS was used as a threshold and indicated by blue lines, after which the space was divided into the three areas A-C. The red line indicates the infiltration in which a saturated zone was formed after equilibrium was reached in IQS as shown in Fig. 8, and after the G.L.-0.8 m value increased in area A, the G.L.-1.0 m value increased, after which it took a trajectory toward area

C. The purple line represents the five rainfall events that reached saturation without an equilibrium state in IQS, including that shown in Fig. 9. All trajectories went from area A to area C. Within area C, the rate of increase of the G.L.-1.0 m value tended to be larger than that of G.L.-0.8 m, and even after the increase in the G.L.-1.0 m value stopped, the G.L.-0.8 m value continued to increase. Note that the trajectory within area A is not uniform.

Finally, we conducted a comparison with the rainfall infiltration status discriminant diagram [11] (jgs2023 Nakayama) for site A. For site A, when rainfall infiltration exceeded D-IQS, the trajectory when vertical rainfall was predominant was $A\rightarrow B\rightarrow A$, and the trajectory when lateral inflow was predominant was $A\rightarrow C\rightarrow A$, and thus the trajectories shown in Figs. 11 and 13 for site B are different. That is, the trajectory patterns are different between the discriminant diagrams for sites A and B.

4.2 Verification of Versatility of Discriminant Diagram

The results of comparing and verifying the rainfall infiltration situation obtained from the discriminant diagram and the infiltration situation obtained from the observation results in Section 3 are as follows.

- (1) The infiltration in Section 3(a) can be understood from the discriminant diagram in Fig. 11. The trajectory within area A can be used to understand whether vertical infiltration or lateral inflow was predominant above the strata boundary.
- (2) The infiltration in Section 3(b) is indicated by the trajectory not reaching area C in the discriminant diagram of Fig. 11. If there is an event that reaches area C in the future, saturation will have reached a depth of G.L.-0.4 m, and it could be concluded that an unprecedented increase in pore water pressure resulted in decreased effective stress and increased risk of slope failure.
- (3) The infiltration in Section 3(c) could be understood from the discriminant diagram in Fig. 13. The saturated zone was rising as the trajectory of the

discriminant diagram went from area A to area C. If the G.L.-0.8 m value continued to rise even after the G.L.-1.0 m value stopped increasing, then it could be inferred that G.L.-1.0 m was saturated.

(4) It is difficult to determine whether the equilibrium state according to the IQS described in Section 3(d) was occurring or not using the discriminant diagram. However, using D-IQS as the threshold of the discriminant diagram enabled easy determination of the rainfall infiltration situation.

5. Conclusion

The observation results were limited, but the following main findings were obtained.

- (1) In the surface layer halfway up the slope face of site B, there was lateral inflow at the top of the strata boundary, and it was inferred that there was lateral inflow similar to site A occurring with the rain that fell on the track area.
- (2) In cases where a saturated zone formed at the installation depth of the soil moisture meter, then the D-IOS could be estimated from the observation data.
- (3) The rainfall infiltration situation estimated from the simple discriminant diagram matches the rainfall infiltration situation estimated from the change over time in volumetric water content. This and the results from site A demonstrate the versatility of the simple determination method using rainfall infiltration status discriminant diagrams.
- (4) The results of site A and site B show that the rainfall infiltration status could be easily understood from the rainfall infiltration status discriminant diagram using D-IQS as the threshold. However, the pattern of the trajectory varies depending on the thickness of the embankment and the sedimentation environment.

In the future, we will collect field monitoring data targeting embankments that are built by filling in valleys and mountain streams and are susceptible to water intrusion, and embankments that are installed in plain areas and do not have spring water. We will also work on reproduction experiments using laboratory slope model experiments and increase the number of locus patterns in the discriminant diagrams. We aim to use this as a basis for building a system that allows even inexperienced engineers to determine the rainfall infiltration situation in real-time.

Acknowledgments

We thank the members of the Osaka University Slope Disaster Prevention Research Group (at the time) and C. S. Inspector Co., Ltd. for their assistance with field monitoring, and Earth Watch Institute, Inc. for their assistance with collecting observation data.

References

- [1] Kojima, K. 2014. "Design and Maintenance of Railway Soil Structures." *The Japanese Geotechnical Society* 62 (7): 10-1.
- [2] Taya, S., and Midorikawa, S. 2016. "An Estimation Method of Train Suspension Periods due to Earthquake." *Journal of Japan Association for Earthquake Engineering* 16 (9): 67-85.
- [3] Nunokawa, O., Sugiyama, T., Mori, T., Ota, N., and Okada, K. 2009. "A Method of Predicting the Scale of Rainfall-Related Embankment and Cut Slope Collapse by Statistical Analysis." *Journal of Japan Society of Civil Engineers* 65 (3): 728-44.
- [4] BBC. 2024. "Hook Landslip: Rail Disruption Ends as Line Reopens after Repairs." Accessed April 27, 2024. https://www.bbc.com/news/uk-england-hampshire-64749 185.
- [5] Kate, T., and Andy, G. 2024. "Repair Team Faces Huge Rail Embankment Challenge." Accessed April 27, 2024. https://www.bbc.com/news/articles/cev905nwp7xo.
- [6] AFPBB News. 2023. "Train Derails in Sweden, Injuring 3 People Train Derails in Sweden due to Heavy Rain, Injuring 3 People Heavy Rains Wash Away Track

- Embankment." Accessed April 27, 2024. https://www.afpbb.com/articles/-/3476217.
- [7] Railway Technical Research Institute. 2007. Maintenance Standards for Railway Structures and Commentary (Earth Structures). Maruzen: Railway Technical Research Institute, pp. 70-4.
- [8] Shimamura, H. 1989. "Revision of Train Operation Regulation Code for Train Operation during Heavy Rainfall and Increase of River Water." *Journal of Japan Railway Civil Engineering Association* 22 (6): 37-40.
- [9] Koizumi, K., Komatsu, M., Oda, K., Ito, S., and Tsutsumi, H. 2021. "A Consideration for Evaluating of Slope Health Monitoring during Rainfall Focusing on Volumetric Water Content." *Journal of Japan Society of Civil Engineers* 77 (2): 129-39.
- [10] Hara, T., Kondo, T., Ishikawa, K., Nakayama, T., and Koizumi, K. 2023. "Research on Rainfall Penetration by Volume of Railway Embankments (Part 1 Local Ground Investigation)." In *Proceedings of the 58th Japan National* Conference on Geotechnical Engineering, July 11-14, 2023.
- [11] Nakayama, T, Hara, T., Ishikawa, K., Kondo, T., and Koizumi, K. 2023. "Research on Rainfall Infiltration of Railway Embankments (Part 2 Field Observation)." In Proceedings of the 58th Japan National Conference on Geotechnical Engineering, July 11-14, 2023.
- [12] Ishikawa, K., Hara, T., Kondo, T., Nakayama, T., and Koizumi, K. 2023. "Research on Rainfall Infiltration of Rail-Way Embankments (Part3 Column Test)." In Proceedings of the 58th Japan National Conference on Geotechnical Engineering, July 11-14, 2023.
- [13] Nakayama, T., Hara, T., Ishikawa, K., and Koizumi, K. 2022. "Rainfall Infiltration Characteristics of Railway Embankments Based on Field Monitoring." In Proceedings of the 11th International Symposium on Field Monitoring in Geomechanics, September 4-8, 2022, London, UK, pp. 1-7.
- [14] Ishikawa, K., Hara, T., Nakayama, T., and Koizumi, K. 2022. "Behavior of Rainfall and Moisture Content by Volume of Railway Embankments (Part 1 Soil Test)." In *Proceedings of the 57th Annual Meeting of Japan National Conference on Geotechnical Engineering*, pp. 5-6.